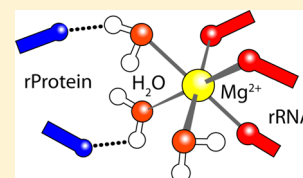


RNA–Magnesium–Protein Interactions in Large Ribosomal Subunit

Anton S. Petrov,^{†,§} Chad R. Bernier,^{‡,§} Chiaolong Hsiao,^{‡,§} C. Denise Okafor,^{‡,§}
Emmanuel Tannenbaum,^{‡,§} Joshua Stern,^{†,§} Eric Gaucher,^{†,§} Dana Schneider,^{‡,§} Nicholas V. Hud,^{‡,§}
Stephen C. Harvey,^{†,‡,§} and Loren Dean Williams^{‡,§,*}

[†]School of Biology, [‡]School of Chemistry and Biochemistry, and [§]NAI Center for Ribosomal Origins and Evolution, Georgia Institute of Technology, Atlanta, Georgia 30332, United States

ABSTRACT: Some of the magnesium ions in the ribosome are coordinated by multiple rRNA phosphate groups. These magnesium ions link distal sequences of rRNA, primarily by incorporating phosphate groups into the first coordination shell. Less frequently, magnesium interacts with ribosomal proteins. Ribosomal protein L2 appears to be unique by forming specific magnesium-mediated interactions with rRNA. Using optimized models derived from X-ray structures, we subjected rRNA/magnesium/water/rProtein L2 assemblies to quantum mechanical analysis using the density functional theory and natural energy decomposition analysis. The combined results provide estimates of energies of formation of these assemblies, and allow us to decompose the energies of interaction. The results indicated that RNA immobilizes magnesium by multidentate chelation with phosphate, and that the magnesium ions in turn localize and polarize water molecules, increasing energies and specificities of interaction of these water molecules with L2 protein. Thus, magnesium plays subtle, yet important, roles in ribosomal assembly beyond neutralization of electrostatic repulsion and direct coordination of RNA functional groups.



■ INTRODUCTION

The ribosome, responsible for the synthesis of coded proteins, is an RNA-protein machine found in all living organisms. Three-dimensional structures of ribosomes from many species have been determined,^{1–6} providing a treasure trove of structural information on RNA folding and interactions, including information on the roles of ribosomal RNA (rRNA), inorganic ions, and ribosomal proteins (rProteins).

The ribosome is a ribozyme—rProteins are not directly involved in catalysis.^{5,7} However, rProteins play critical roles in many aspects of ribosomal assembly and function.^{8,9} Globular domains of rProteins are confined to the surfaces of the subunits, while polypeptide extensions of idiosyncratic conformation penetrate into the subunit cores. Many of the interactions between rRNA and the rProtein extensions are simply Coulombic: rProtein extensions contain cationic side chains that interact electrostatically with anionic phosphate groups of the rRNA.

We are interested in interactions between rProteins and inorganic cations that associate with the rRNA. Compaction of RNA, as during assembly of the ribosome, requires inorganic cations. Magnesium was seen early on to be important in tRNA folding.^{10–12} It is now known that magnesium plays a special role in folding of essentially all large RNAs.^{13–16} Highly coordinated magnesium ions are seen here to mediate interactions between rRNA and rProteins. An elaborate network of rRNA, magnesium ions, water molecules, and rProtein L2 form part of the scaffold for the peptidyl transferase center (PTC) (Figure 1A). We demonstrate that the specific properties of magnesium^{17–20} are critical to the stability of these networks. We subjected structural components of the network to quantum mechanical analysis using the density functional theory, and determined how magnesium-mediate

interactions between the rRNA and rProtein. The results show that magnesium ions chelated by rRNA activate water molecules for molecular recognition of rProteins. Magnesium-activated water molecules are integral to the folded ribosome.

■ METHODS

rProtein L2 Sequence Retrieval and Alignment.

rProtein L2 sequences from 121 species with fully sequenced genomes were selected^{21–23} and aligned. All eukaryotic kingdoms are represented in this sequence data set. Of the 30 recognized phyla of bacteria,²⁴ 14 are included in the data set. Of the 5 recognized phyla of archaea, 3 are included. Within the selected archaean phyla, every class is represented. Sequences were retrieved from the NCBI database using BLASTP,²⁵ and were aligned with COBALT,²⁶ a constraint-based alignment tool for multiple protein sequences. The alignments were visually inspected. Domain of life-specific sequence blocks that could not be aligned between domains were removed.

D2-AMN Crystal Structures. Coordinates of the D2-AMN complex (Figure 1B) were extracted from the crystal structure of the *Thermus thermophilus* (*T. thermophilus*) ribosome (PDB ID: 2J00, chain Z, and ID: 2J01, chains A and D). The D2-AMN complex consists of amino acid residues Ala 225, Met 226, and Asn 227 from rProtein L2, and magnesium microcluster D2, which composed of two magnesium ions, Mg 66 and Mg 70, first shell water molecules, and two short fragments of 23S rRNA that interact with the magnesium ions

Received: May 15, 2012

Revised: June 18, 2012

Published: June 19, 2012

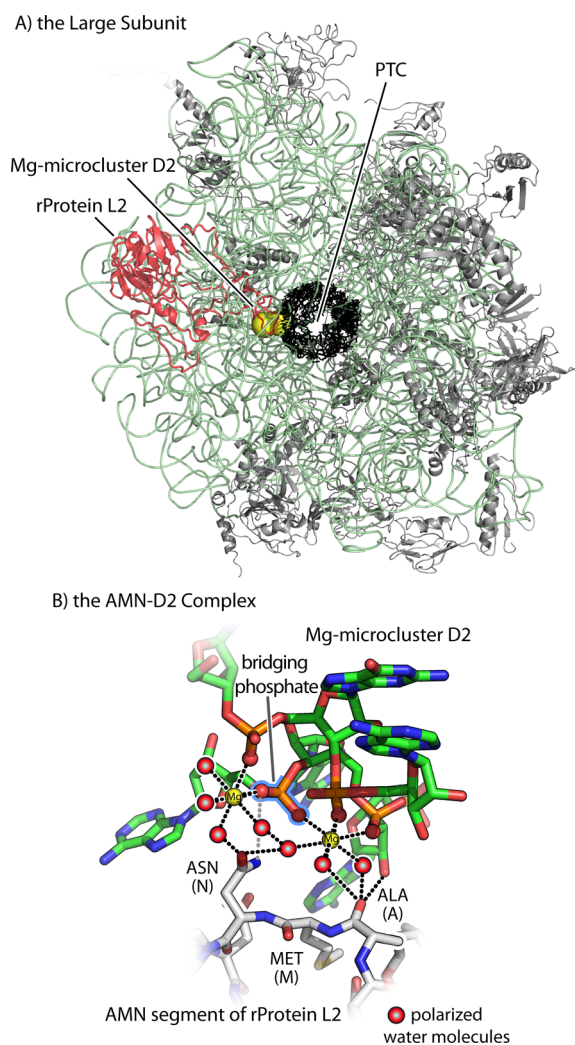


Figure 1. (A) The LSU from *Thermus thermophilus*, viewing directly into the PTC. rProtein L2 (red ribbon) is composed of a globular domain on the surface of the LSU and an extension that penetrates deep into the interior. The 23S rRNA is indicated by a green ribbon. The two magnesium ions of Mg- μ C D2, that associate with rProtein L2, are indicated by yellow spheres. Other ribosomal proteins of the LSU are shown in gray ribbon. The rRNA that lines the peptide exit tunnel is highlighted in black. (B) An atomic level view of the interactions of the 23S rRNA, the AMN fragment of rProtein L2 and the two magnesium ions (yellow spheres) of Mg- μ C D2. Hydrogen bonds and first shell interactions of the magnesium ions with water or phosphate are shown as dashed lines. The bridging phosphate, that interacts with two magnesium ions is highlighted in blue. Ribosomal RNA is colored green (carbon), red (oxygen) and blue (nitrogen). The AMN fragment of rProtein L2 is colored white (carbon), red (oxygen), blue (nitrogen), and yellow (sulfur). Oxygens in the first coordination shell of magnesium are indicated by small spheres, whose radii have no physical significance. The coordinates of this complex were extracted from a crystal structure of the LSU (PDB ID: 2J01).

(ADE 783, GUA 784, and GUA 2588, ADE 2589) as shown in Figure 1B. Structural elements used to computationally build up the D2-AMN complex are shown in Figure 2A–E. The intact D2-AMN complex is shown in Figure 3A.

D2-AMN Models. Hydrogen atoms, first shell water molecules of the magnesium ions as well as the –OH group added in the C terminus of the AMN peptide were optimized, while the heavy atoms were fixed in the positions of the crystal structures (Figure 3A). The optimization used the b3lyp/6-31+

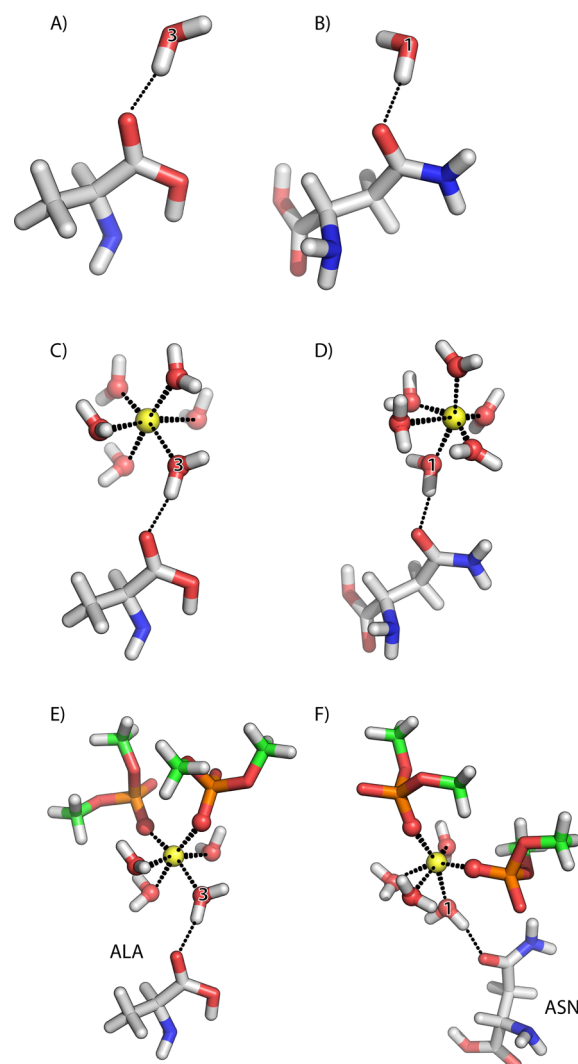


Figure 2. Building up the D2-AMN complex. (A) The amino acid Ala 225 interacts with water molecule W3. The water molecule is linked to the amino acid by one hydrogen bond. (B) Complex of the amino acid Asn 227 with water molecule W1, linked by one hydrogen bond. (C) Complex of the amino acid Ala 225 with water molecule W3, with one hydrogen bond. W3 is polarized by insertion into the first shell of a magnesium ion. (D) Complex of the amino acid Asn 227 with water molecule W1, with one hydrogen bond. W2 is polarized by insertion into the first shell of a magnesium ion. (E) A hydrogen bonded complex of the amino acid Ala 225 with magnesium first shell water molecule W3. The magnesium ion is chelated by two phosphate oxygens from the rRNA. (F) Complex of the amino acid Asn 227 with magnesium first shell water molecule W1. The magnesium is chelated by two phosphate oxygens. Atoms are colored as in Figure 1B.

+G(d,p) level of theory in the Gaussian 03 suite of programs.²⁷ Positions of water molecules were initially modeled using the water positions of the LSU of *Haloarcula marismortui* (PDB ID: 1JJ2). Although the D2-AMN complexes are virtually indistinguishable in the two structures,²⁸ the *H. marismortui* ribosome is of higher resolution and contains more detail in the hydration layer than the *T. thermophilus* ribosome. The (H₂O)₄-AMN complex (Figure 3B) was extracted from D2-AMN without further geometry optimization. The interaction energies for all complexes were calculated as a difference between the single point energies of a complex and its monomers in the gas phase at the b3lyp/6-311++G(d,p) level

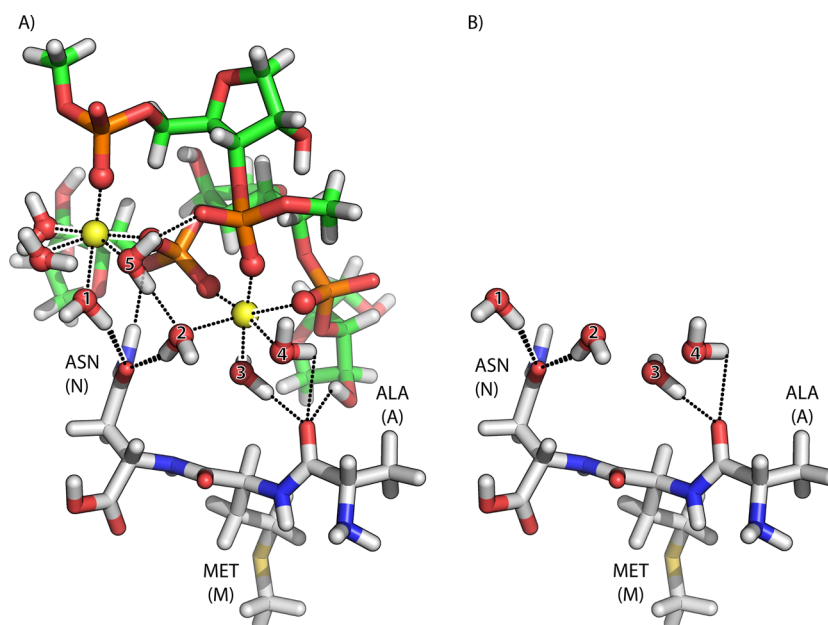


Figure 3. RNA–magnesium–water–protein assemblies investigated here by calculation. (A) The D2-AMN complex ($\text{Mg-}\mu\text{c D2} + \text{AMN}$) is composed of rRNA, two magnesium ions, seven water molecules and the AMN fragment of rProtein L2. Magnesium ions and their first shell water molecules mediate interactions between the rRNA and the AMN fragment of rProtein L2. Water molecules are oriented and polarized by the magnesium ions, interacting strongly with AMN. In this model system, the phosphodiester backbone of the rRNA is terminated by O-methyl groups. Bases are replaced by hydrogen atoms. (B) Interactions of four nonpolarized water molecules with ribosomal protein L2. The $(\text{H}_2\text{O})_4\text{-AMN}$ complex characterized here is formed by omitting the magnesium ions and the rRNA from D2-AMN. Water molecules W1–W4 were extracted from the first hydration shells of magnesium ions. The atoms are colored as in Figure 1B.

of theory, and are reported with the 50% correction^{29,30} for the Basis Set Superposition Error (BSSE) using the counterpoise procedure of Boys and Bernardi.³¹ The D2-AMN complex is buried within the LSU, and not exposed to the bulk water. This complex is located in an area with relatively low dielectric coefficient. Therefore, all calculations reported here are performed in gas phase, and neglect the polarization effects of the bulk solvent.

Stepwise building up of D2-AMN. Complexes X–Y (with X = subset of the atoms of $\text{Mg-}\mu\text{c D2}$, and Y = peptide AMN, or amino acids Ala or Asn) were constructed. The parent structure, with X = D2 and Y = AMN is the optimized D2-AMN complex (Figure 3A). Other X–Y complexes contain omissions of appropriate atoms and are capped with hydrogen atoms and –OH groups where necessary to maintain correct valence. Dimethyl phosphates ($_{\text{DM}}\text{P}^-$) were used to model RNA phosphate groups. We describe what amounts to a construction process, a series of partial complexes that are converted in a stepwise fashion to the parental complex D2-AMN. This approach is akin to the Auf Bau process, but on a molecular scale. The series of complexes of increasing size and complexity can be seen in Figure 2.

The smallest complexes, denoted $\text{H}_2\text{O-Y}$ [Figure 2A (Y = Ala) and 2B (Y = Asn)], were created by extracting an amino acid (Ala or Asn) and a water molecule hydrogen bonded to the amino acid from the previously optimized D2-AMN complex. To generate the isolated amino acids, peptide bonds were cleaved and the amino acid residues were capped appropriately with –OH or –H groups. The $\text{H}_2\text{O-Y}$ complexes were not further optimized. The interaction energies for this and all other complexes were calculated at the b3lyp/6-311++G(d,p) level of theory as a difference between energies for the

X–Y complexes and the separated components with 50% of BSSE. Relaxation energies of monomers were neglected.

A second pair of complexes, denoted $\text{Mg}(\text{H}_2\text{O})_6^{2+}\text{-Y}$ [Figure 2C (Y = Ala) and 2D (Y = Asn)] were created by extracting $\text{Mg}(\text{H}_2\text{O})_4^{2+}\text{-Y}$ from the parental D2-AMN complex, and replacing the two omitted first shell phosphates with first shell water molecules. These water molecules were optimized at the b3lyp/6-311++G(d,p) level of theory, while other atoms were fixed.

A third set of complexes, denoted $[(_{\text{DM}}\text{P}^-)_2\text{-Mg}(\text{H}_2\text{O})_4^{2+}]\text{-Y}$ [Figure 2E (Y = Ala) and 2F (Y = Asn)] was created by extracting the atoms of the appropriate amino acid, magnesium ion, four water molecules, and two phosphate groups from D2-AMN. The phosphate groups were capped with 3' and 5' methyl groups. Newly added atoms were subjected to optimization at the b3lyp/6-311++G(d,p) level of theory, while the portions extracted from the D2-AMN complexes were kept fixed.

NBO and NEDA Analyses. Partitioning of the total (TOT) interaction energy (IE) into electrostatic (EL), polarization (POL), charge transfer (CT), steric exchange (EX), and deformational (DEF) energy components was performed according to the Natural Bond Orbital (NBO) and Natural Energy Decomposition Analyses (NEDA) scheme implemented in the GAMESS package³² using NBO 5.9 routine.^{33–35} Some advantages of the NEDA scheme are that it provides a direct measure of the degree of polarization of charge distributions, satisfies the Pauli exclusion principle, and has been successfully applied to study interactions between cations of alkaline-earth metals and water molecules.³⁶ The NBO charge calculations and the energy decomposition were performed for all complexes using the following levels: b3lyp/6-31+G(d,p) for the D2-AMN complexes; b3lyp/6-311++G(d,p)

for the $(\text{H}_2\text{O})_4\text{-AMN}$, $[(\text{DM}^{\text{P}^-})_2\text{-Mg}(\text{H}_2\text{O})_4]^{2+}\text{-Y}$, $\text{Mg}(\text{H}_2\text{O})_6^{2+}\text{-Y}$, and $\text{H}_2\text{O-Y}$ complexes.

RESULTS

The highest resolution X-ray structures of ribosomes indicate over a hundred magnesium ions are closely associated with the large ribosomal subunit (LSU).^{3,37} Among these magnesium ions are a subset within a motif called the magnesium microcluster ($\text{Mg-}\mu\text{c}$).^{28,38,39} Four $\text{Mg-}\mu\text{c}$'s (called $\text{Mg-}\mu\text{c}$ D1, $\text{Mg-}\mu\text{c}$ D2, $\text{Mg-}\mu\text{c}$ D3, and $\text{Mg-}\mu\text{c}$ D4) are conserved in position and interactions in archaeal and bacterial LSUs, and appear to be conserved throughout the tree of life.^{28,40}

A $\text{Mg-}\mu\text{c}$ contains two closely associated Mg^{2+} ions that are directly coordinated by one or more common phosphate group(s) in the form $\text{Mg}^{2+}_{(\text{a})}\text{-(OP-P-OP)-Mg}^{2+}_{(\text{b})}$ where OP-P-OP indicates a part of the phosphate group that bridges between the two magnesium ions. The bridging phosphate of $\text{Mg-}\mu\text{c}$ D2 is highlighted in Figure 1B. Both magnesium ions of a $\text{Mg-}\mu\text{c}$ contain additional phosphate groups in their first shells. $\text{Mg-}\mu\text{c}$'s appear to provide structural integrity to the LSU and help maintain the compact native structure of the assembly.

rRNA, Mg^{2+} , water, and rProtein L2. Here, we focus on $\text{Mg-}\mu\text{c}$ D2, one of three magnesium microclusters located in close proximity to the PTC. $\text{Mg-}\mu\text{c}$ D2 consists of Mg 66 and Mg 70 (in *T. thermophilus*, PDB ID: 2J01), which form the nucleus of an intricate interaction network. The first coordination shells of these magnesium ions contain in total five phosphate oxygens from the rRNA [ADE 783 and GUA 784 (Domain II) and GUA 2588 and ADE 2589 (Domain V)] and seven water molecules. Four of these water molecules interact directly with rProtein L2. The complete assembly, D2-AMN, consists of $\text{Mg-}\mu\text{c}$ D2 and three amino acids (AMN) of rProtein L2 (Figure 1B). Inspection of LSU three-dimensional structures reveals that in comparison with other rProteins, L2 makes the most extensive interactions with Mg^{2+} ions. The positions of the backbone atoms of this segment of rProtein L2 appear to be highly conserved throughout the tree of life.²⁸

rProtein L2 Sequence Conservation. The amino acids of rProtein L2 that interact with $\text{Mg-}\mu\text{c}$ D2 show modest sequence variability in various organisms. Sequence alignment of L2 from 121 species, distributed over all three domains of life, suggests that sequences of this tripeptide fall into nine possible amino acid triads (shown in Table 1). The most frequent triad is AMN (as seen in L2 of *T. thermophilus*), which is observed in 78/121 organisms surveyed (65%). The most

Table 1. Composition of rProtein L2 Amino Acid Sequences That Interact with Mg^{2+} Ions in $\text{Mg-}\mu\text{c}$'s in the Large Ribosomal Subunit Based on the Sequences of 121 Organisms

L2-fragment	count	fraction
AMN	78	0.644
VMN	28	0.231
AMS	4	0.033
AKN	3	0.024
ARN	2	0.016
KMN	2	0.016
SMN	2	0.016
CMN	1	0.008
KKN	1	0.008
Sum	121	1.000

frequent amino acid at position 1 is Ala (Ala 225, 72%); the most frequent amino acid at position 2 is Met (Met 226, 95%); and the most frequent amino acid at position 3 is Asn (Asn 227, 97%). The sequence Ala or Val (225) at position 1, Met (226) at position 2, and Asn (227) at position 3 highly dominate available sequences. The residue numbers listed here and throughout the text are based on the rProtein L2 of *T. thermophilus*, because the length of L2 varies between species.

Energetics of Deconstructed Complexes. We have previously used quantum methods to characterize rRNA–magnesium and DNA–water–magnesium complexes.^{39,41} Extending that approach here, we dissect the complexes, first breaking them down to single amino acids bound to single water molecules, then building up to the complete network. The complexes characterized here are shown in Figure 2. We analyze the stability of each complex, revealing the effects of magnesium ions and the phosphate groups on the hydrogen bonds between the amino acid residues and water molecules.

The interaction energies of the $\text{H}_2\text{O-Y}$ complexes (Figure 2A and 2B), each of which contains one $\text{O-H}\cdots\text{O}$ hydrogen bond, are -5.2 kcal/mol for Ala, and -5.2 kcal/mol for Asn. The BSSE corrected interaction energies for all these complexes are listed in Table 2. These values are in reasonable agreement with conventional estimates of $\text{O-H}\cdots\text{O}$ hydrogen bond energies.⁴² NEDA decomposition for this set of complexes is provided in Table 3.

Table 2. 50% BSSE Corrected Interaction Energies for $\text{H}_2\text{O-Y}^{\text{a}}$, $\text{Mg}(\text{H}_2\text{O})_6^{2+}\text{-Y}^{\text{a}}$ and $[(\text{DM}^{\text{P}^-})_2\text{-Mg}(\text{H}_2\text{O})_4]^{2+}\text{-Y}^{\text{a}}$ Complexes (kcal/mol)

Y	$\text{H}_2\text{O-Y}^{\text{b}}$	$\text{Mg}(\text{H}_2\text{O})_6^{2+}\text{-Y}^{\text{b}}$	$[(\text{DM}^{\text{P}^-})_2\text{-Mg}(\text{H}_2\text{O})_4]^{2+}\text{-Y}^{\text{b}}$
Ala	-5.2	-21.8	-13.4
Asn	-4.5	-20.7	-15.2

^aY indicates an amino acid, either Ala or Asn. ^bEnergies are obtained at the b3lyp/6-311++G(d,p)//b3lyp/6-311++G(d,p) level of theory.

The interaction energy of a water molecule with an amino acid is significantly enhanced if the water molecule is inserted into the first shell of a magnesium ion (Figure 2C,D and Table 2). NEDA analysis (Table 3) indicates that the stability of the $\text{Mg}(\text{H}_2\text{O})_6^{2+}\text{-Y}$ complexes is increased by electrostatic, polar-

Table 3. Natural Energy Decomposition Analysis for $\text{H}_2\text{O-Y}^{\text{a}}$, $\text{Mg}(\text{H}_2\text{O})_6^{2+}\text{-Y}^{\text{a}}$ and $[(\text{DM}^{\text{P}^-})_2\text{-Mg}(\text{H}_2\text{O})_4]^{2+}\text{-Y}^{\text{a}}$ Complexes (kcal/mol)

complex ^b	EL ^c	POL ^c	CT ^c	EX ^c	DEF ^c	TOT ^c
$\text{H}_2\text{O-Ala}$	-11.1	-6.4	-15.9	-4.2	32.8	-4.9
$\text{H}_2\text{O-Asn}$	-14.0	-6.7	-21.5	-5.1	43.2	-4.1
$\text{Mg}(\text{H}_2\text{O})_6^{2+}\text{-Ala}$	-17.9	-15.3	-22.4	-3.6	37.6	-21.5
$\text{Mg}(\text{H}_2\text{O})_6^{2+}\text{-Asn}$	-18.9	-15.6	-28.9	-4.5	47.6	-20.3
$[(\text{DM}^{\text{P}^-})_2\text{-Mg}(\text{H}_2\text{O})_4]^{2+}\text{-Ala}$	-16.4	-8.1	-18.5	-3.8	33.9	-12.9
$[(\text{DM}^{\text{P}^-})_2\text{-Mg}(\text{H}_2\text{O})_4]^{2+}\text{-Asn}$	-20.4	-10.3	-30.3	-5.7	52.4	-14.3

^aY indicates an amino acid, either Ala or Asn. ^bEnergies and NEDA components are obtained at the b3lyp/6-311++G(d,p)//b3lyp/6-311++G(d,p) level of theory. ^cElectrostatic (EL), polarization (POL), charge-transfer (CT), exchange (EX), deformational (DEF) components, and the total interaction energy (TOT) are calculated in the framework of the NEDA scheme.

ization, and charge transfer effects. The interaction energies are -21.8 kcal/mol for $\text{Mg}(\text{H}_2\text{O})_6^{2+}$ -Ala, and -20.7 kcal/mol for $\text{Mg}(\text{H}_2\text{O})_6^{2+}$ -Asn.

To establish the effects of phosphate groups within the magnesium first shell on the hydrogen bonding interaction energies, we calculated the interaction energies for the complexes $[(\text{DM}^{\text{P}^-})_2\text{-Mg}(\text{H}_2\text{O})_4^{2+}]\text{-Y}$ as shown in Figures 2E and 3F and Table 2. The stability of the $[(\text{DM}^{\text{P}^-})_2\text{-Mg}(\text{H}_2\text{O})_4^{2+}]\text{-A}$ is -13.4 kcal/mol, and that of the $[(\text{DM}^{\text{P}^-})_2\text{-Mg}(\text{H}_2\text{O})_4^{2+}]\text{-N}$ complex is -15.2 kcal/mol. A comparison of the energies of these complexes with those for $\text{Mg}(\text{H}_2\text{O})_6^{2+}\text{-X}$ reveals a drop in interaction energy when the phosphate groups are inserted into the magnesium first shell. The electrostatic, polarization, and charge transfer components of the interaction energies (Table 3) are all attenuated by the phosphate groups. Thus, RNA phosphate groups decrease the polarization effect by magnesium ions, and destabilize the complexes between these amino acids and water molecules. Nevertheless, the strength of the interactions remain significantly greater than those for $\text{H}_2\text{O}\text{-Y}$. The enhancement of the water–protein interaction by magnesium ions is not fully abrogated by the phosphate groups.

A magnesium ion, even with two phosphate oxygens in its first shell, transfers charge from first shell water molecules. Consequently, these first shell water molecules form relatively strong hydrogen bonds, pulling charge from the atoms of amino acids to which they form hydrogen bonds (see the detailed discussion on the charge transfer below). Thus, charge is transferred from the amino acids via water molecules to magnesium ions by a relay mechanism, which enhances the stability of the $[(\text{DM}^{\text{P}^-})_2\text{-Mg}(\text{H}_2\text{O})_4^{2+}]\text{-Y}$ complexes. Overall, our results reveal that the magnesium ions coordinated by rRNA play an important role not only in connecting remote regions of RNA molecule but also in stabilizing RNA–protein interactions.

Stability of D2-AMN and $(\text{H}_2\text{O})_4\text{-AMN}$ Complexes. We have characterized the full D2-AMN complex (rRNA–magnesium–water–protein), which consists of $\text{Mg}\text{-}\mu\text{c}$ D2 in association with the AMN segment of rProtein L2. The initial coordinates of D2-AMN, along with appropriate neighboring nucleotides, were extracted from the crystal structure of the *T. thermophilus* ribosome, and optimized. The optimized structure, including hydrogen atoms, is shown in Figure 3A. The interaction energies for D2-AMN calculated at the b3lyp/6-311++G(d,p)//b3lyp/6-31++G(d,p) level of theory is -42.9 kcal/mol (Table 4).

The first amino acid of AMN, Ala 225, forms three hydrogen bonds with $\text{Mg}\text{-}\mu\text{c}$ D2 via the carbonyl oxygen of the peptide backbone (Figure 3A). Two of those hydrogen bonds are with water molecules (W3 and W4) and one is with a 2'-hydroxyl oxygen of the rRNA. The side chain of Asn 227, the third amino acid of AMN, forms two hydrogen bonds with first shell

water molecules (W1 and W2) of a magnesium ion of $\text{Mg}\text{-}\mu\text{c}$ D2 and one hydrogen bond with a phosphate oxygen of the rRNA.

To confirm the importance of the magnesium ions in the stability of the D2-AMN complex, we omitted the rRNA and the magnesium ions from the complexes, and recalculated the interaction energies between the peptide triads and the remaining four water molecules. After this omission, the magnesium ions no longer polarize the water molecules. The interaction energies for the $(\text{H}_2\text{O})_4\text{-AMN}$ complex (Figure 3B) are -9.9 kcal/mol (Table 4), which are significantly lower than the energies of those interactions in the intact D2-AMN complex. This result is consistent with our analysis above, and confirms that magnesium ions activate water molecules located in their first shell and enhance the stability of the D2-AMN complex by up to 4-fold compared to the $(\text{H}_2\text{O})_4\text{-AMN}$ complex, even though they do not interact directly with the protein.

Energy Decomposition of D2-AMN and $(\text{H}_2\text{O})_4\text{-AMN}$ Complexes. Overall, the water–rProtein interaction energies of the three complexes are roughly predicted by the number of hydrogen bonds between rProtein L2 and $\text{Mg}\text{-}\mu\text{c}$ D2. However, the magnitudes of the D2-AMN interaction energies are greater than expected by summing the conventional estimates for four $\text{O}\cdots\text{H}\cdots\text{O}$ hydrogen bonds [$\sim 3.0\text{--}5.0$ kcal/mol each⁴³]. Results from Natural Energy Decomposition Analysis of D2-AMN (Table 5), indicate that the stability of the complex appears to

Table 5. Natural Energy Decomposition Analysis for D2-AMN and $(\text{H}_2\text{O})_4\text{-AMN}$ Complexes (kcal/mol)

complex ^a	EL ^b	POL ^b	CT ^b	EX ^b	DEF ^b	TOT ^b
D2-AMN	−55.4	−39.1	−94.2	−15.5	165.6	−38.6
$(\text{H}_2\text{O})_4\text{-AMN}$	−34.6	−19.3	−72.2	−12.9	130.6	−8.4

^aTotal NEDA energies and NEDA components are obtained at the b3lyp/6-31+G(d,p)//b3lyp/6-31++G(d,p) level of theory. ^bElectrostatic (EL), polarization (POL), charge-transfer (CT), exchange (EX), deformational (DEF) components and the total interaction energy (TOT) are calculated in the framework of the NEDA scheme.

arise from favorable electrostatic, charge transfer and polarization components, opposed by unfavorable deformational energy (all terms of the interaction energy discussed here are defined within the framework of NEDA scheme; the meaning of the terms can be found elsewhere^{33–35}).

Polarization. The rRNA and magnesium ions enhance the stability of the D2-AMN complex without directly interacting with the rProtein. This effect is seen by analysis of an analogous complex that omits the rRNA and the magnesium ions, in the form of $(\text{H}_2\text{O})_4\text{-AMN}$ (Figure 3B). This omission causes the water molecules to depolarize, attenuating the interaction energy. As shown by the results of the NEDA analysis (Table 5) the polarization component in the D2-AMN complex (-39.1 kcal/mol) is substantially larger than that in the $(\text{H}_2\text{O})_4\text{-AMN}$ complex (-19.3 kcal/mol). Thus, the polarization of water molecules by the magnesium ions plays a significant role in the stability of the rRNA–magnesium–water–protein complexes. Our result here is consistent with previous observations that the pK_a of water molecules decrease upon incorporation into the magnesium first shell.¹⁹

Charge Transfer. Charge transfer makes important contributions to stability to the D2-AMN complex (NEDA analysis is summarized in Table 5). The total charge on AMN in the

Table 4. Interaction Energies (IE) and 50% BSSE Corrected Interaction Energies for D2-AMN and $(\text{H}_2\text{O})_4\text{-AMN}$ Complexes (kcal/mol)

complex ^a	IE	IE (BSSE)
D2-AMN	−37.5	−42.9
$(\text{H}_2\text{O})_4\text{-AMN}$	−8.6	−9.9

^aEnergies are obtained at the b3lyp/6-311++G(d,p)//b3lyp/6-31++G(d,p) level of theory.

Table 6. NBO Charges (e), H-Bond Distances (\AA), and the Values of the Energy Lowering Due to Charge Transfer $\Delta E_{(n \rightarrow \sigma^*)}$ (kcal/mol) for D2-AMN and $(\text{H}_2\text{O})_4$ -AMN Complexes

unit	charge (e) in D2-AMN	charge (e) in $(\text{H}_2\text{O})_4$ -AMN	H-bond atoms	distance (\AA)	$\Delta E_{(n \rightarrow \sigma^*)}$ D2-AMN	$\Delta E_{(n \rightarrow \sigma^*)}$ $(\text{H}_2\text{O})_4$ -AMN
D2* ^a	−0.1472					
AMN	0.10885	0.06573				
W1	−0.01643	−0.02996	OD(N227)⋯O—H (W1)	1.710	19.2	16.9
W2	0.03364	−0.01233	OD(N227)⋯O—H (W2)	1.835	10.3	8.7
W3	−0.00651	−0.02524	O(A225)⋯O—H (W3)	1.748	17.2	15.4
W4	0.02765	0.00179	O(A225)⋯O—H (W4)	3.284		
total WAT	0.03835	−0.6573			46.7	41.0

^aThe D2* complex is a subset of the Mg- μ c D2 complex as shown in Figure 3A, without four water molecules W1–W4, which are treated separately in this analysis.

D2-AMN complex (0.1088 e) drops when the RNA and magnesium ions are removed (0.06573 e , Table 6). Mg^{2+} ions and their first shell water molecules mediate charge transfer from the protein by 0.04307 e (65%) compared to in the $(\text{H}_2\text{O})_4$ -AMN complex. The charges of water molecules W1 (−0.0164 e) and W3 (−0.0065 e) in the D2-AMN complex are significantly smaller than those in the $(\text{H}_2\text{O})_4$ -AMN complex (W1, −0.0299 e ; W3, −0.02524 e ; Table 6). Thus, these water molecules act simultaneously as electron donors and acceptors, with a net reduction of their net charges. Such behavior, according to the Weinhold theory,⁴⁴ indicates cooperative charge transfer, and suggests that the charge transfer occurs by a relay mechanism from the proteins via bridging waters to the magnesium ions.

Cooperative charge transfer is not indicated for W2 or W4. The difference between W1 and W3 versus W2 and W4 is partially explained by their geometries. W1 and W3 are properly oriented for formation of strong H-bonds with AMN. The distance between the OD atom of Asn 227 and the H atom of W1 is 1.710 \AA and that between the O atom of Ala 225 and the H atom of W3 is 1.748 \AA . The H-bond between the H atom of W2 and the OD atom of Asn 227 is somewhat longer, leading to a reduction of charge transfer. Additionally, W2 also serves as an H-bond acceptor, forming an H-bond with W5 (Figure 3A). This additional hydrogen bond results in more complicated path of the charge transfer for W2 and loss in the cooperative effect. W4 is located much further from the AMN peptide (the distance between the O atom of Ala 225 and the H atom of W4 is 3.284 \AA) and does not play a significant role in the stabilization of the D2-AMN complex.

This explanation of the charge transfer mechanism in terms of geometrical considerations is supported by the quantitative characterization of the energies associated with the charge transfer. Table 6 contains the largest values of the energy lowering due to the charge transfer ($E_{n \rightarrow \sigma^*}$) from two lone pairs of each of the oxygen atoms of the AMN (the O atom of Ala 225 and the OD atom of Asn 227) to the vacant σ^* orbitals of the water molecules as revealed by NEDA. The largest values of these energies are found to be 19.2 kcal/mol for W1 and 17.2 kcal/mol for W3. Similar values in the $(\text{H}_2\text{O})_4$ -AMN complexes are only 16.9 and 15.4 kcal/mol. The energy lowering for W2 is lower compared to those for W1 and W3, and is 10.3 kcal/mol for D2-AMN complex and 8.7 for $(\text{H}_2\text{O})_4$ -AMN complex. Thus, the cooperative charge transfer between the proteins and magnesium ions mediated by water molecules plays a significant role in enhancing stability of the D2-AMN complex.

DISCUSSION

The ribosome can be viewed as a molecular fossil, with structural and functional characteristics dating back to ancient life.^{40,45–48} RNA, proteins, ions, and water molecules within the ribosome combine to form intricate networks that have been interpreted as time-stamps of evolution. Fox,⁴⁵ Steinberg,⁴⁶ Yonath,^{49,50} Hsiao,⁴⁰ Noller,⁵¹ and others agree that the part of Domain V containing the peptidyl transferase center (PTC) is the oldest component of the LSU, with later incorporation of elements allowing for interaction with the small subunit (SSU). Yonath and co-workers have proposed that the contemporary peptidyl transferase center is a relic of an early proto-ribosome.⁵⁰ Hsiao et al. have described an “onion” method of ribosomal analysis, in which the LSU is sectioned into concentric shells, using the peptidyl transferase center as the origin.⁴⁰ This approach allows quantitative and statistical analysis of various structural characteristics, with the assumption that, on average, regions more distant from the PTC correspond to more recent additions to the ribosome.

It is known that magnesium plays a special role in RNA folding in general.^{13,14,37,38} Magnesium shares a special geometric and electrostatic complementarity with oxygen atoms, forming a rigid and tightly packed octahedral.^{52,53} Magnesium draws oxyanions of adjacent phosphates into direct proximity in complexes stabilized not only by electrostatic interactions but also by charge transfer, polarization, and exchange.³⁹ Magnesium is therefore involved in distinctive conformational and energetic states of RNA.^{28,39} Magnesium ions link remote regions of the rRNA, by incorporating remote phosphate groups into the magnesium first coordination shell.^{28,37}

In the core of the ribosome, the 23S rRNA forms many first shell interactions with magnesium ions,³⁷ in some cases fixing their positions by chelation. A subset of chelated magnesium ions appears to be universally conserved over phylogeny.²⁸ First shell water molecules that coordinate these highly conserved magnesium ions interact with the extension of rProtein L2, which is one of the most highly conserved ribosomal proteins⁵⁴ and one of the ‘early’ rProteins in the Neirhaus assembly map.⁵⁵

The magnesium microcluster Mg- μ c D2 contains two magnesium ions that are bridged by a RNA phosphate²⁸ and coordinated by both rRNA phosphate groups and water molecules. Mg- μ c D2 is associated with three amino acids of rProtein L2 in the D2-AMN complex. Magnesium links rRNA to protein by orienting and polarizing water molecules within the magnesium first coordination shell. These magnesium first shell waters interact strongly with protein. Other available biological cations such as sodium, cationic amino acids or polyamines, do not polarize and orient water molecules to the

same extent and therefore could not substitute for magnesium in functional ribosomes. Located in close proximity to the PTC of the LSU and linking secondary Domains II and V of the 23S rRNA, the D2-AMN complex appears to be important in ribosomal architecture, but not catalysis. No atoms of D2-AMN are sufficiently close to the site of peptide bond formation for participation in catalysis.

Three consecutive amino acids of rProtein L2 form hydrogen bonds with water molecules of the first hydration shells of two adjacent magnesium ions. The backbone atoms of Ala 225 and Met 226 and the side chain atoms of Asn 227 of rProtein L2 form hydrogen bonds with these activated water molecules. As indicated in part by close similarities between ribosomal structures from the primary branches of the tree of life, this part of ribosome appears to have remained nearly invariant over vast evolutionary time.^{28,40} Conservation of Mg- μ c D2 between archaea and bacteria includes rRNA and magnesium positions and interactions, and extends to the positions and orientations of the magnesium first-shell water molecules. Additionally, the high degree of conservation of Ala 225, Met 226, and Asn 227 in rProtein L2 is observed across the phylogenetic tree. Therefore, the D2-AMN complex appears to be a critical component of one of the oldest assemblies in the biological world.

CONCLUSIONS

In the current work, we discussed the factors affecting the stability of the highly conserved rRNA/magnesium/water/rProtein L2 complex located in the central region of the ribosomal LSU. We examined the natural sequence variation of the fragment of rProtein L2 that interacts with Mg- μ c D2. We subjected structures of the consensus sequence (AMN) to quantum mechanical analysis using the density functional theory to characterize interactions and conformations within the ribosome. Our deconstruction and computational results show that the magnesium ions in Mg- μ c D2 enhance the interactions of water molecules with L2 protein.

By performing a detailed analysis of the interaction components in the D2-AMN complex and its derivatives, we have identified previously unrecognized non-Coulombic charge transfer and polarization components important to the stability of rRNA/magnesium/water/protein complexes. The water molecules that link rProtein L2 to Mg ions in the Mg- μ c D2 cluster are polarized due to their close proximity to magnesium ions. These water molecules also mediate charge transfer from rProtein L2 to magnesium ions by a charge relay mechanism. Both of these factors substantially enhance the stability of rRNA/magnesium/water/rProtein L2 assemblies. The energetics of specifically bound magnesium ions and RNA are not treated accurately by Molecular Dynamics (MD), nonlinear Poisson–Boltzmann or other continuum theories,^{39,56–60} in part due to “nonelectrostatic” components of the interactions. Quantum mechanics methods are required for an accurate description of these interactions.

AUTHOR INFORMATION

Corresponding Author

*E-mail: loren.williams@chemistry.gatech.edu.

Notes

The authors declare no competing financial interest.

ACKNOWLEDGMENTS

We thank Dr. David Sherrill and Ms. Jessica Bowman for helpful discussions. This work was supported by the NASA Astrobiology Institute (NNA09DA78A)

REFERENCES

- (1) Rabl, J.; Leibundgut, M.; Ataide, S. F.; Haag, A.; Ban, N. *Science* **2011**, *331*, 730.
- (2) Ben-Shem, A.; Jenner, L.; Yusupova, G.; Yusupov, M. *Science* **2010**, *330*, 1203.
- (3) Selmer, M.; Dunham, C. M.; Murphy, F. V.; Weixlbaumer, A.; Petry, S.; Kelley, A. C.; Weir, J. R.; Ramakrishnan, V. *Science* **2006**, *313*, 1935.
- (4) Harms, J.; Schlutzen, F.; Zarivach, R.; Bashan, A.; Gat, S.; Agmon, I.; Bartels, H.; Franceschi, F.; Yonath, A. *Cell* **2001**, *107*, 679.
- (5) Ban, N.; Nissen, P.; Hansen, J.; Moore, P. B.; Steitz, T. A. *Science* **2000**, *289*, 905.
- (6) Cate, J. H.; Yusupov, M. M.; Yusupova, G. Z.; Earnest, T. N.; Noller, H. F. *Science* **1999**, *285*, 2095.
- (7) Noller, H. F.; Hoffarth, V.; Zimniak, L. *Science* **1992**, *256*, 1416.
- (8) Klein, D. J.; Moore, P. B.; Steitz, T. A. *J. Mol. Biol.* **2004**, *340*, 141.
- (9) Wilson, D. N.; Nierhaus, K. H. *Crit. Rev. Biochem. Mol. Biol.* **2005**, *40*, 243.
- (10) Stein, A.; Crothers, D. M. *Biochemistry* **1976**, *15*, 160.
- (11) Lynch, D. C.; Schimmel, P. R. *Biochemistry* **1974**, *13*, 1841.
- (12) Lindahl, T.; Adams, A.; Fresco, J. R. *Proc. Natl. Acad. Sci. U. S. A.* **1966**, *55*, 941.
- (13) Brion, P.; Westhof, E. *Annu. Rev. Biophys. Biomol. Struct.* **1997**, *26*, 113.
- (14) Draper, D. E. *Biophys. J.* **2008**, *95*, S489.
- (15) Auffinger, P.; Grover, N.; Westhof, E. *Met. Ions Life Sci.* **2011**, *9*, 1.
- (16) Bowman, J. C.; Lenz, T. K.; Hud, N. V.; Williams, L. D. *Curr. Opin. Struct. Biol.* **2012**, in press.
- (17) Petrov, A. S.; Funseth-Smotzer, J.; Pack, G. R. *Int. J. Quantum Chem.* **2005**, *102*, 645.
- (18) Markham, G. D.; Glusker, J. P.; Bock, C. W. *J. Phys. Chem. B* **2002**, *106*, 5118.
- (19) Baes, C. F.; Mesmer, R. E. *Hydrolysis of Cations*; Wiley: New York, 1976.
- (20) Serdyuk, I. N.; Zaccai, N. R.; Zaccai, J. *Methods in Molecular Biophysics: Structure, Dynamics, Function*; Cambridge University Press: Cambridge, UK, 2007.
- (21) Gaucher, E. A.; Govindarajan, S.; Ganesh, O. K. *Nature* **2008**, *451*, 704.
- (22) Blair Hedges, S.; Blair, J.; Venturi, M.; Shoe, J. *BMC Evol. Biol.* **2004**, *4*, 1.
- (23) Gribaldo, S.; Brochier, C. *Res. Microbiol.* **2009**, *160*, 513.
- (24) Euzéby, J. P. *Int. J. Syst. Bacteriol.* **1997**, *47*, 590.
- (25) Altschul, S. F.; Madden, T. L.; Schaffer, A. A.; Zhang, J.; Zhang, Z.; Miller, W.; Lipman, D. J. *Nucleic Acids Res.* **1997**, *25*, 3389.
- (26) Papadopoulos, J. S.; Agarwala, R. *Bioinformatics* **2007**, *23*, 1073.
- (27) Frisch, M. J.; Trucks, G. W.; Schlegel, H. B.; Scuseria, G. E.; Robb, M. A.; Cheeseman, J. R.; Montgomery, J. A.; Vreven, T.; Kudin, K. N.; Burant, J. C.; Millam, J. M.; Iyengar, S. S.; Tomasi, J.; Barone, V.; Mennucci, B.; Cossi, M.; Scalmani, G.; Rega, N.; Petersson, G. A.; Nakatsuji, H.; Hada, M.; Ehara, M.; Toyota, K.; Fukuda, R.; Hasegawa, J.; Ishida, M.; Nakajima, T.; Honda, Y.; Kitao, O.; Nakai, H.; Klene, M.; Li, X.; Knox, J. E.; Hratchian, H. P.; Cross, J. B.; Bakken, V.; Adamo, C.; Jaramillo, J.; Gomperts, R.; Stratmann, R. E.; Yazyev, O.; Austin, A. J.; Cammi, R.; Pomelli, C.; Ochterski, J. W.; Ayala, P. Y.; Morokuma, K.; Voth, G. A.; Salvador, P.; Dannenberg, J. J.; Zakrzewski, V. G.; Dapprich, S.; Daniels, A. D.; Strain, M. C.; Farkas, O.; Malick, D. K.; Rabuck, A. D.; Raghavachari, K.; Foresman, J. B.; Ortiz, J. V.; Cui, Q.; Baboul, A. G.; Clifford, S.; Cioslowski, J.; Stefanov, B. B.; Liu, G.; Liashenko, A.; Piskorz, P.; Komaromi, I.; Martin, R. L.; Fox, D. J.; Keith, T.; Al-Laham, M. A.; Peng, C. Y.; Nanayakkara, A.; Challacombe, M.; Gill, P. M. W.; Johnson, B.; Chen,

W.; Wong, M. W.; Gonzalez, C.; Pople, J. A. *Gaussian 03, Revision E.01*; Gaussian, Inc.: Wallingford, CT, 2004.

- (28) Hsiao, C.; Williams, L. D. *Nucleic Acids Res.* **2009**, *37*, 3134.
- (29) Kim, K. S.; Tarakeshwar, P.; Lee, J. Y. *Chem. Rev.* **2000**, *100*, 4145.
- (30) Barrientos, C.; Sordo, J. *Theor. Chem. Acc.* **2007**, *118*, 733.
- (31) Boys, S. F.; Bernardi, F. *Mol. Phys.* **1970**, *19*, 553.
- (32) Gordon, M. S.; Schmidt, M. W. Advances in Electronic Structure Theory: Gamess a Decade Later. In *Theory and Applications of Computational Chemistry: The First Forty Years*; Dykstra, C. E., Frenking, G., Kim, K. S., Scuseria, G. E., Eds.; Elsevier: Amsterdam, 2005.
- (33) Glendening, E. D.; Streitwieser, A. *J. Chem. Phys.* **1994**, *100*, 2900.
- (34) Glendening, E. D. *J. Am. Chem. Soc.* **1996**, *118*, 2473.
- (35) Schenter, G. K.; Glendening, E. D. *J. Phys. Chem.* **1996**, *100*, 17152.
- (36) Glendening, E. D.; Feller, D. *J. Phys. Chem.* **1996**, *100*, 4790.
- (37) Klein, D. J.; Moore, P. B.; Steitz, T. A. *RNA* **2004**, *10*, 1366.
- (38) Hsiao, C.; Tannenbaum, M.; VanDeusen, H.; Hershkowitz, E.; Perng, G.; Tannenbaum, A.; Williams, L. D. Complexes of Nucleic Acids with Group I and II Cations. In *Nucleic Acid Metal Ion Interactions*; Hud, N., Ed.; The Royal Society of Chemistry: London, 2008; pp 1.
- (39) Petrov, A. S.; Bowman, J. C.; Harvey, S. C.; Williams, L. D. *RNA* **2011**, *17*, 291.
- (40) Hsiao, C.; Mohan, S.; Kalahar, B. K.; Williams, L. D. *Mol. Biol. Evol.* **2009**, *26*, 2415.
- (41) Petrov, A. S.; Lamm, G.; Pack, G. R. *J. Phys. Chem. B* **2002**, *106*, 3294.
- (42) Jeffrey, G. A. *An Introduction to Hydrogen Bonding*; Oxford University Press: New York, 1997.
- (43) Jeffrey, G. A.; Saenger, W. *Hydrogen Bonding in Biological Structures*; Springer-Verlag: New York, 1991.
- (44) Weinhold, F. *J. Mol. Struct.: THEOCHEM* **1997**, 398–399, 181.
- (45) Fox, G. E. *Cold Spring Harb. Perspect. Biol.* **2010**, *2*, a003483.
- (46) Bokov, K.; Steinberg, S. V. *Nature* **2009**, *457*, 977.
- (47) Smith, T. F.; Lee, J. C.; Gutell, R. R.; Hartman, H. *Biol. Direct.* **2008**, *3*, 16.
- (48) Wolf, Y. I.; Koonin, E. V. *Biol. Direct.* **2007**, *2*, 14.
- (49) Krupkin, M.; Matzov, D.; Tang, H.; Metz, M.; Kalaora, R.; Belousoff, M. J.; Zimmerman, E.; Bashan, A.; Yonath, A. *Philos. Trans. R Soc. London, Ser. B: Biol. Sci.* **2011**, *366*, 2972.
- (50) Belousoff, M. J.; Davidovich, C.; Zimmerman, E.; Caspi, Y.; Wekselman, I.; Rozenszajn, L.; Shapira, T.; Sade-Falk, O.; Taha, L.; Bashan, A.; Weiss, M. S.; Yonath, A. *Biochem. Soc. Trans.* **2010**, *38*, 422.
- (51) Noller, H. F. *Cold Spring Harb. Perspect. Biol.* **2010**, *7*, 7.
- (52) Brown, I. D. *Acta Crystallogr., Sect. B.* **1992**, *48*, 553.
- (53) Bock, C. W.; Markham, G. D.; Katz, A. K.; Glusker, J. P. *Theor. Chem. Acc.* **2006**, *115*, 100.
- (54) Meskauskas, A.; Russ, J. R.; Dinman, J. D. *Nucleic Acids Res.* **2008**, *7*, 7.
- (55) Rohl, R.; Nierhaus, K. H. *Proc. Natl. Acad. Sci. U.S.A.* **1982**, *79*, 729.
- (56) Gresh, N.; Sponer, J. E.; Spackova, N.; Leszczynski, J.; Sponer, J. *J. Phys. Chem. B* **2003**, *107*, 8669.
- (57) Rulisek, L.; Sponer, J. *J. Phys. Chem. B* **2003**, *107*, 1913.
- (58) Petrov, A. S.; Pack, G. R.; Lamm, G. *J. Phys. Chem. B* **2004**, *108*, 6072.
- (59) Petrov, A. S.; Lamm, G.; Pack, G. R. *Biopolymers* **2005**, *77*, 137.
- (60) Anthony, P. C.; Sim, A. Y.; Chu, V. B.; Doniach, S.; Block, S. M.; Herschlag, D. *J. Am. Chem. Soc.* **2012**, *134*, 4607.